Visual Abstract

Improvement of crack tip position estimation in DIC images by image processing methods

Zekriti Najat, Majid Fatima, Hachimi Taoufik
Laboratory of Nuclear, Atomic, Molecular, Mechanical and Energetic Physics, Chouaib Doukkali University, El jadida, Morocco
najat.ze@hotmail.fr; majidfatima9@gmail.com; hachtaoufik@gmail.com

Tounsi Yassine
Measurement and Control Instrumentation Laboratory IMC, Chouaib Doukkali University, El Jadida, Morocco
yassinetounsi132@gmail.com

Rhanim Rajaa
Laboratory Study of Advanced Materials and Application, University Moulay Ismail, Meknes, Morocco
rajaaarhanim@gmail.com

Mrani Ibrahim, Rhanim Hassan
Laboratory of Nuclear, Atomic, Molecular, Mechanical and Energetic Physics, Chouaib Doukkali University, El jadida, Morocco
ibmrani@gmail.com, rhanimhassan@hotmail.com

ABSTRACT. The study proposes and compares two procedures to identify the crack tip location in PVC Sent samples under a uniaxial tensile test based on the image processing method.
An IDS camera captures several photos of the PVC surface as part of the image analysis procedure. All relevant data on crack initiation and propagation is collected and assessed using ImageJ software using image processing methods for detecting cracks.
However, the second procedure involves a developed algorithm detecting the discontinuity using digital image correlation (DIC) measurement. Although, because of the experimental conditions, the acquisition of images by the digital camera is never perfect. This noise comes from several sources, including the digital camera, image distortion due to lens magnification or lens angle, the shape and size of the pattern, and electronic noise; ... This article discusses image enhancement methods to overcome these objectionable characteristics using and comparing several filters: Gaussian, median, and Unsharp Mask filters. The performance of the Gaussian filter is better than the Median and Unsharp mask filters. This research demonstrates that DIC is an effective technique for monitoring deformation and understanding the failure mechanism with the best-suited filter.

OPEN ACCESS

Citation: Najat, Z., Majid, F., Taoufik, H., Tounsi, Y., Rhanim, R., Mrani, I., Rhanim, H., Improvement of crack tip position estimation in DIC images by image processing methods, Frattura ed Integrità Strutturale, 63 (2023) 61-71.

Received: 29.08.2022
Accepted: 06.10.2022
Online first: 22.10.2022
Published: 01.10.2023

KEYWORDS. Crack tip location, full-field data, ImageJ, DIC, PVC, Gaussian filter, Median filter, Unsharp Mask filter.

INTRODUCTION

The detection of the crack tip location appears to be a vital issue in the communities involved in predicting the behavior of materials and structures [1]–[3] as long as the initiation and propagation of cracks frequently impact the usability of engineering structures and components during their lifetime.[4], [5]. on the one hand, this is due to the singularity of the mechanical fields at the crack tip and, on the other hand, to the problems heightened by detecting the crack tip location and propagation.[6], [7]. An overview of the literature in this area reveals that numerous investigations have been conducted to identify cracks in different types of materials. Various techniques can determine the crack tip position and propagation, assisted by a camera, X-ray diffraction, ultrasonic, and laser-based methods.[8]–[10]. Crack identification based on image processing techniques is advantageous for providing an accurate quantitative result over traditional methods.[11]

In this context, Rasband[12] has developed the open-source software ImageJ based on the image analysis method often used in our field to perform image segmentation to isolate and measure the crack. [13], [14]. Cinar et al. proposed a new phase congruence-based crack detection method (PC-CD) to segment and identify cracks, including length, path, and opening displacement profile.[15]. Amongst these image processing methods, the DIC technique has been proposed by Sutton and Chu [16]–[19] as a non-contact optical method to measure the kinematic fields. This technique allows the investigation of crack tip position and propagation from full-field displacements.[20].

To introduce DIC to a large scientific community, Blaber et al. developed a freely available open-source 2D subset-based digital image correlation software (Ncorr).[21], [22]. Using the field displacement data (U_x and U_y) obtained from Ncorr, Harilal et al. converted the non-linear least square problem into a sequence of linear least square problems. They proposed a new algorithm to predict the position of the crack tip[23]. Besides, using the same program, a new algorithm was developed by Marae-Djouda to locate the crack tip in SENT specimens, with the hypothesis that, in the vicinity of the crack, the deformation peaks at its maximum at the crack tip.[24]–[26]. When a camera or other imaging system acquires an image, The vision system it is destined for is usually not directly able to use. Poor contrast, random intensity variations, or variations in illumination can all generate disturbance in an image, which must be dealt with in the initial steps of visual processing. [27], [28]The displacements and deformations computed by DIC are also affected by noise, which is affected by dark noise, photon noise, and read noise.[29], [30] Thus, the filtering method is used to enhance and denoise the image.

In the image processing field, various approaches have been introduced for image filtering [31]. These approaches can be classified into three families: Spatial domain filtering, frequency domain filtering, and hybrid approaches [31].

This paper aims to identify the crack location of PVC Single edge notched tensile (SENT) specimens under a uniaxial tensile test using a digital image process. The article is structured as follows: the first part briefly described the experimental device and experimental procedure proposing a method of measuring. The second part is dedicated to results, in the first time, we determined the crack tip location using the open-source platform (ImageJ/FIJI) software [32], applying the image processing methods for detecting cracks. Then, an algorithm was developed based on DIC for the exported strain field analysis using the Ncorr program to evaluate the crack tip position. Finally, to overcome the limitation caused by the noise in digital images, an image process method is proposed based on filtering images before applying the DIC method using several filters.

EXPERIMENTAL AND METHODS

Preparation of tensile specimens

The Single Edge Notched Tensile has been used to localize the crack tip using DIC. The structure dimension of the samples is accorded to the ASTM D638 standard. Five specimens have been prepared to carry out the tensile test. The SENT specimens were made from plates fabricated by the compression molding process, laser-cut, then manually pre-cracked by 1mm with a razor blade, with dimensions 100x20x2 mm^3, Fig. 1. Besides, the speckle patterns were created by spraying commercial black paint on each SENT's face in the order of a millimeter. The randomer this pattern is, the more influential the DIC method is.

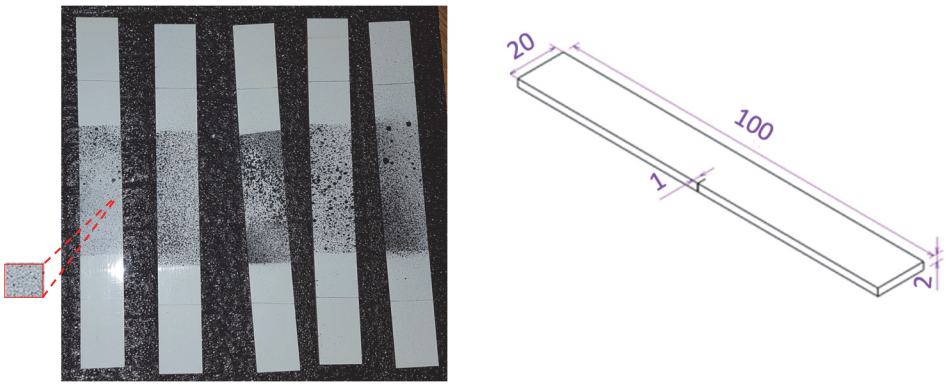

Figure 1: (a) PVC samples with depicted Region Of Interest ROI (b) Dimensions of PVC samples.

Tensile Test

A uniaxial tensile test was performed using a tensile test machine MTS with the maximum 30 kN load capacity and 1020mm/min test speed. The crosshead speed was set as 10 mm/min. The tensile test was registered using an IDS camera UI-3880CP with a full resolution of 3088 x 2076 Pixel and 2.4 µm for pixel size. The experimental field was illuminated by bar light essential 15 blue LEDs +/- 25° with a polarizer to ensure the conditions for capturing images during the tests. The camera's manufacturer set and provided the light so that a uniform intensity was achieved over the specimen's entire illuminated surface. The experimental setup for the tensile test and the stress-strain curve is shown in Fig. 2.

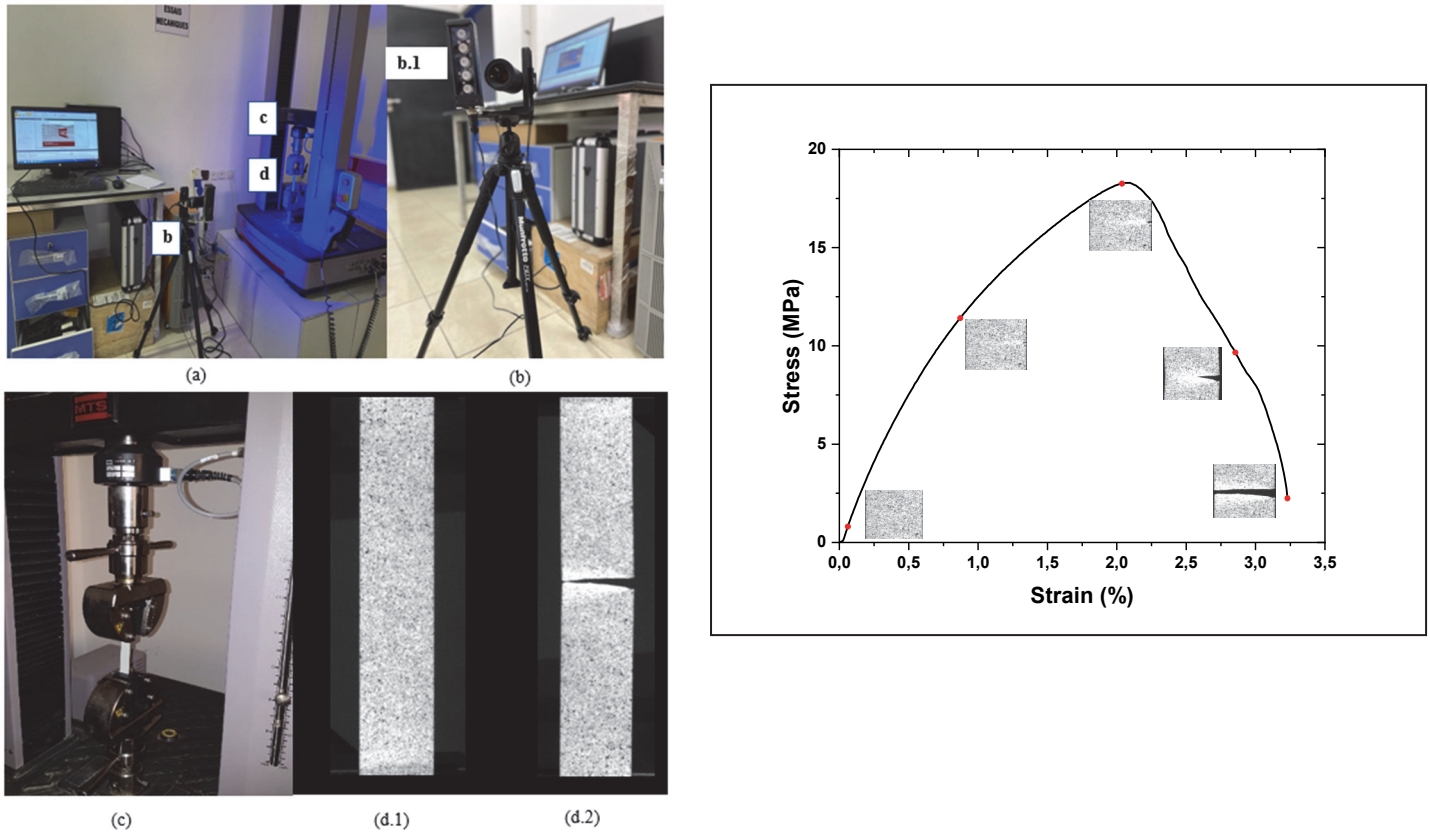

Figure 2: (a)Tensile testing system; (b) DIC system; (b.1) LED Light source; (c)MTS testing machine; (d.1) dumbbell specimen before deformation; (d.2) dumbbell specimen after rupture; (e) Load strain curve.

Digital image correlation

For this method to be relevant, a random pattern is essential over the specimen area. To mathematically identify this pattern, the intensity of each pixel in the reference image and the deformed image must be plotted and then calculated as the displacement vector.

To extract the field of displacement and deformation. In our study, a developed open-source software based on a 2D subset (Ncorr) is used to export the displacement and deformation fields.
In Ncorr, the subsets are primarily a continuous circular group of points on integer pixel positions in the reference configuration. The transformation of the coordinates of these points from the reference to the current configuration is a first-order linear transformation:

$$\begin{aligned} \tilde{x}_{cur_i} &= x_{ref_i} + u_{rc} + \frac{\partial u}{\partial x_{rc}}(x_{ref_i} - x_{ref_c}) + \frac{\partial u}{\partial y_{rc}}(y_{ref_i} - y_{ref_c}) \\ \tilde{y}_{cur_i} &= y_{ref_i} + v_{rc} + \frac{\partial v}{\partial x_{rc}}(x_{ref_i} - x_{ref_c}) + \frac{\partial v}{\partial y_{rc}}(y_{ref_i} - y_{ref_c}) \end{aligned} \quad (i,j) \in S \tag{1}$$

where x_{refi} and y_{refj} are the x and y coordinates of an initial reference subset point, x_{refc} and y_{refc} are the coordinates of the center of the initial reference subset.
Ncorr is using Green-Lagrangian constraints, with the following three displacement gradients generated:

$$E_{xx} = \frac{1}{2}\left(2\frac{\partial u}{\partial x} + \left(\frac{\partial u}{\partial x}\right)^2 + \left(\frac{\partial v}{\partial x}\right)^2\right) \tag{2}$$

$$E_{xy} = \frac{1}{2}\left(\frac{\partial u}{\partial y} + \frac{\partial v}{\partial x} + \frac{\partial u}{\partial x}\frac{\partial u}{\partial y} + \frac{\partial v}{\partial x}\frac{\partial v}{\partial y}\right) \tag{3}$$

$$E_{yy} = \frac{1}{2}\left(2\frac{\partial u}{\partial y} + \left(\frac{\partial u}{\partial y}\right)^2 + \left(\frac{\partial v}{\partial y}\right)^2\right) \tag{4}$$

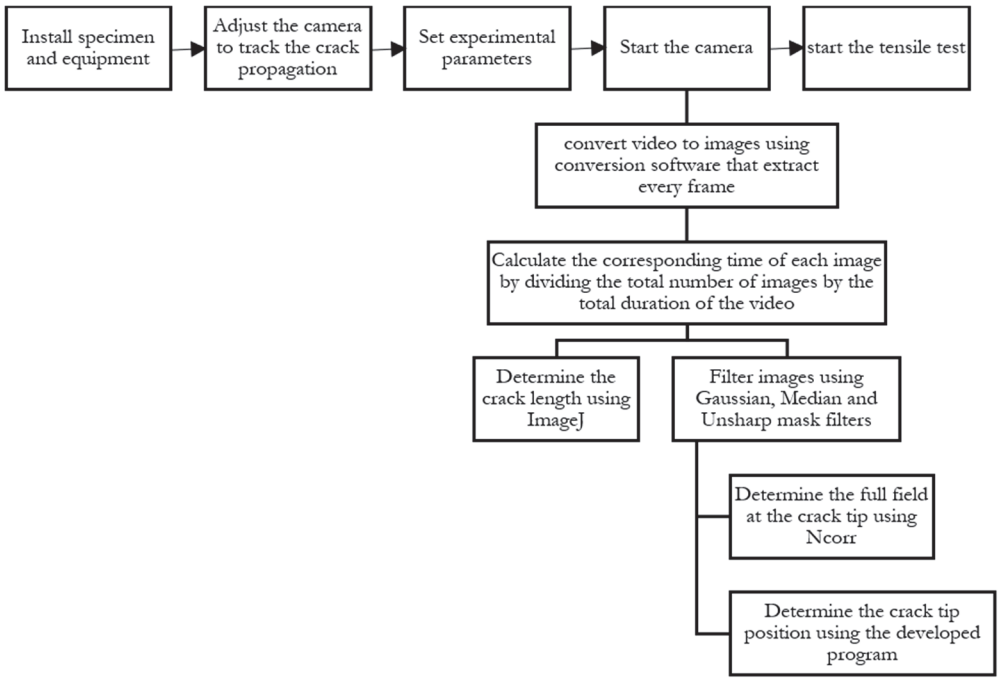

Figure 3: The flowchart of the proposed measuring method.

Identification of crack length

Accurate crack tip position estimation is problematic for fracture mechanics researchers, particularly in the case of materials made of polymers Measuring fracture propagation is challenging in such materials due to extreme necking at the crack tip and considerable plastic deformation.

In this study, two procedures are provided and assessed to detect crack tip location based on image processing methods. The first one is determined by visual identification using ImageJ. The second one uses a developed algorithm applying DIC to the exported strain field analysis. The flowchart of the proposed measuring method is illustrated in Fig. 3.

Filter noise

DIC images are affected by noise whose sources are different. The noise is due to the camera sensor, the structure of the speckle pattern when the preparation, or the non-uniform illumination; in addition, it can be related to software parameters such as the size of the strain window, facet, and step size. In general, the noise still presents in the recorded DIC images, which can affect the quality of the information extraction (i.e., Displacement).

For this reason, a filtering step is essential to remove this noise and, consequently, determine the crack tip position with accuracy.

The DIC process is generally divided into four main steps: Image acquisition, Displacement tracking, Strain analysis, and Data mining. And basically, the smoothing is applied before calculating the strain field because strains implicate differentiation sensitive to noise. In this work, we interfere in the first step by filtering the images before processing them, and we compare the performance of three spatial domain filters for noise removal. This family of filters exploits correlation among the pixels/patches in the noisy image, and the noise removal is realized by an appropriate set of operations on the image matrix.

The first filter is the Gaussian filter; it is a linear filter that exploits the two-dimensional Gaussian function as the mask weight value. The Gaussian function provides a larger weight to the center of the mask, and the weights get attenuated when the distance from the central pixel increases.

The median filter is a nonlinear filter developed to provide a filtered image with less blurring effect. The median filter moves through the image pixel by pixel, replacing each value with the median value of neighboring pixels.

The Unsharp Mask employs a blurred, or "unsharp," negative image to create a mask of the original image to enhance the details. The contrast is then increased, and an image that is less blurry than the original is produced by combining the unsharp mask with the original positive image.

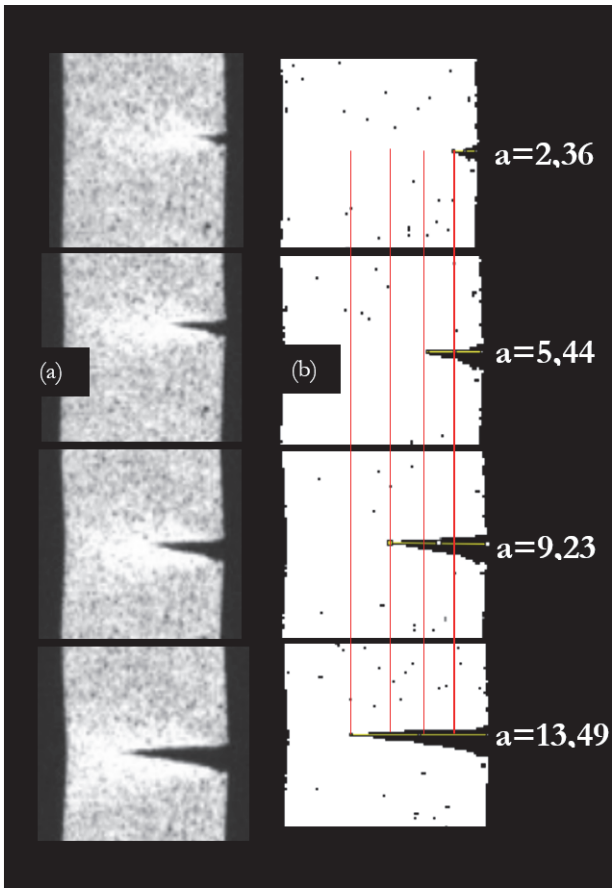

Figure 4: Sequence of images following crack length(a) 8-bit grayscale images acquired during the test; (b) processed images.

RESULTS

Identification of crack tip location - Procedure1: ImageJ

An IDS camera captures several photos of the PVC surface as part of the image analysis procedure. All relevant data on crack initiation and propagation are collected. However, the brightness and reflection of light could not always be consistent. Additionally, surfaces include uneven polish and other noises. To correctly detect the cracks and assess their propagation, it is necessary to analyze the digital images of the surface obtained to remove all of the light variation and noise.

The image processing methods for detecting cracks involve the following steps using the ImageJ software: at first, raw 8-bit grey-level image capture of the desired area of PVC surface, then subtracting the background for uniform brightness, applying Gaussian filter for smoothness, and finally thresholding to track the cracks. Fig. 4 shows the sequence of images to measure the crack length.

After measuring the crack length for all of the processed pictures using ImageJ, the crack length with the corresponding time can be plotted in Fig. 6. a.

The graph shows that the crack initially spreads stationary with a linear shape until taking a parabolic form. Then the crack's growth becomes increasingly out of control, ultimately leading to failure.

Identification of crack tip location – Procedure 2: DIC

To track the crack's growth. The speckled samples, which are centered in the vicinity of the notch tips, are observed using an IDS camera. The numerical data is analyzed using the Ncorr software.

This study proposes an algorithm to monitor crack tip location by utilizing the measured axial deformation near the crack. According to the (x,y) Cartesian frame, considering the crack propagates from right to left, the first zone of discontinuities which is in the area of the fracture process is detected, mains the free zone of deformation expressed by Ncorr by zero value. Therefore, the algorithm developed assumed to find the first zero value in the deformation field after defining the ROI. The main algorithm is described in Fig. 5.

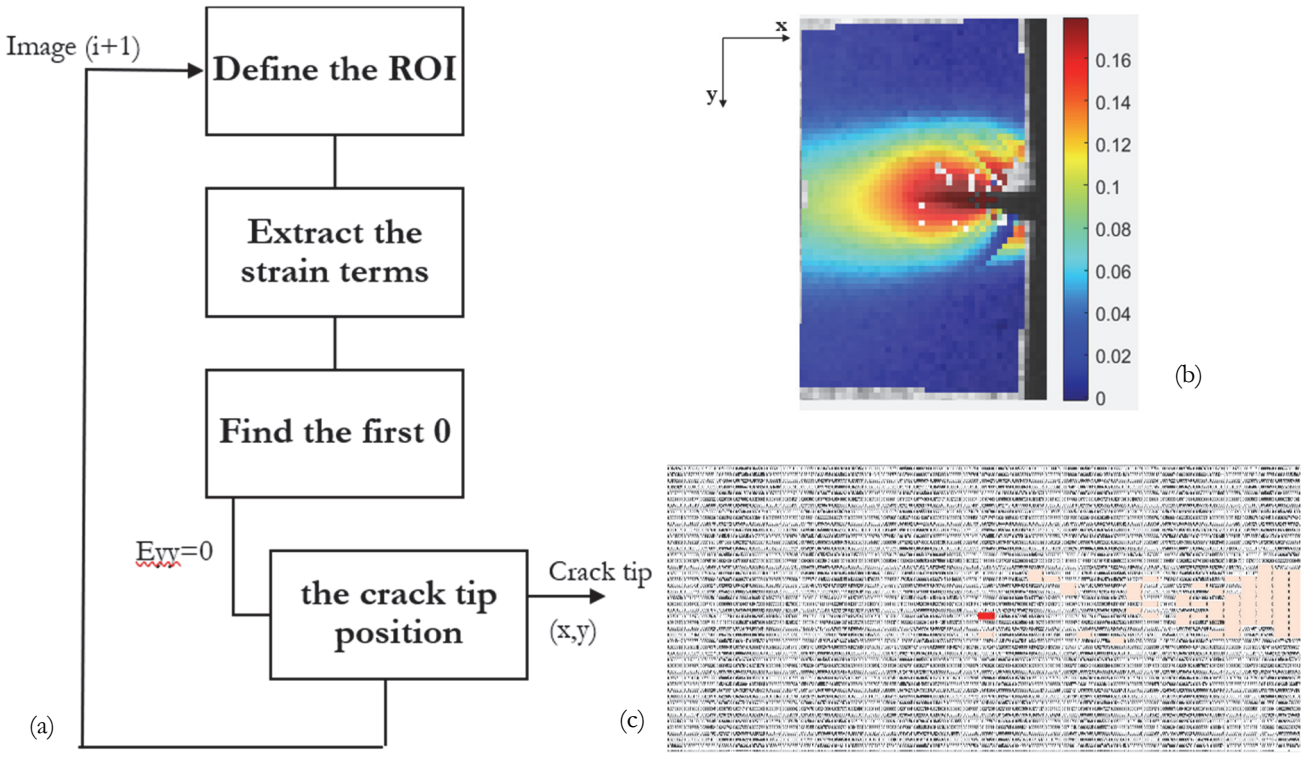

Figure 5: (a) Crack tip location algorithm; (b)Axial strain field at t=33,8s; (c) Axial Strain matrix.

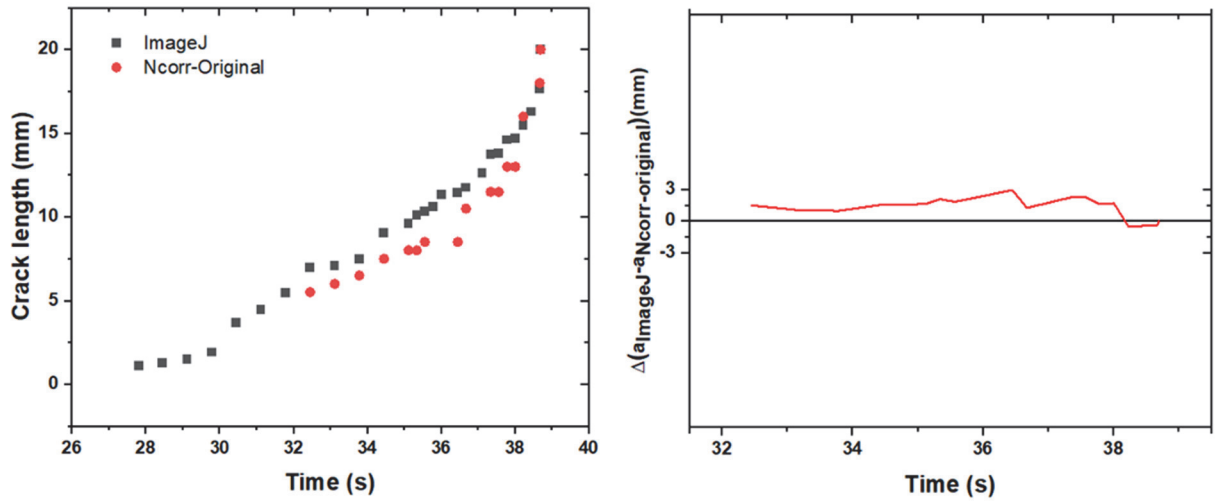

(a) (b)

Figure 6: (a) crack length as a function of time using ImageJ and the developed algorithm; (b) Difference between the two graphs

As seen in the graph above, the crack propagation data was obtained using both methods. At the start of the test, there was no detectable crack propagation. Due to the small displacement range because of the elastic zone, both techniques have uncertainty during the initial stages. In this zone (from 28s to 32,5s), the crack did not cause discontinuities in the measured strain fields due to small displacement. It was found that the first method detected smaller crack lengths than the strain field-based method, despite these low displacement levels. However, the curves do not line up, as seen in Fig. 6. b, which allows us to consider that the measurements in DIC are intrinsically noisy. This noise has numerous factors and affects the detection of discontinuities.

To overcome this limitation, an image process method is proposed based on filtering images before applying the DIC method.

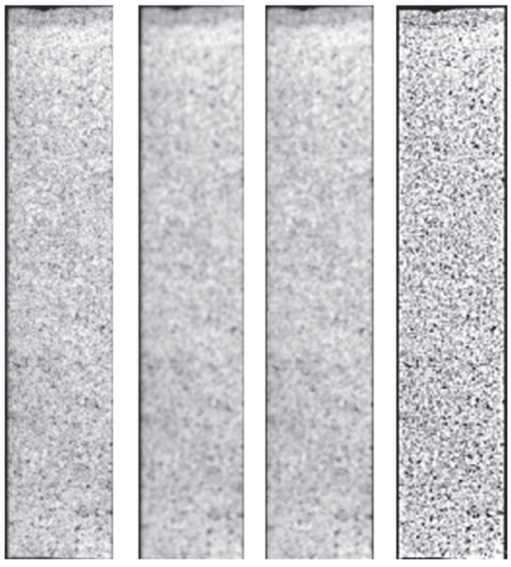

(a) (b) (c) (d)

Figure 7: Visual comparisons of denoising results on PVC sample (a) Original (b) Gaussian filter (c) Median filter (d) Unsharp mask filter.

Comparison of filtering methods

Three filters are applied to remove noise in the DIC images; Fig. 7 summarizes the denoising comparative outcomes for the various filtering techniques. Furthermore, to generate singularity characterizing data from the displacement field, the Ncorr program was used. Fig. 7 gives the deformation field data around the crack tip to illustrate a direct comparison between the

different filters. We can see in the Fig. 9 that the discontinuity and the crack demonstrate a high level of agreement with the Gaussian filter than with the Median filter, where the details of the crack edges are challenging to detect correctly, maybe because the median filter computes each output sample as the median value of the input samples inside the window; the outcome is the median value following the sorted of the input values considering that the edges take zero value. On the other hand, crack detection is almost absent using the Unsharp Mask filter; since the final image is clearer, the subject concept may be less accurately represented.

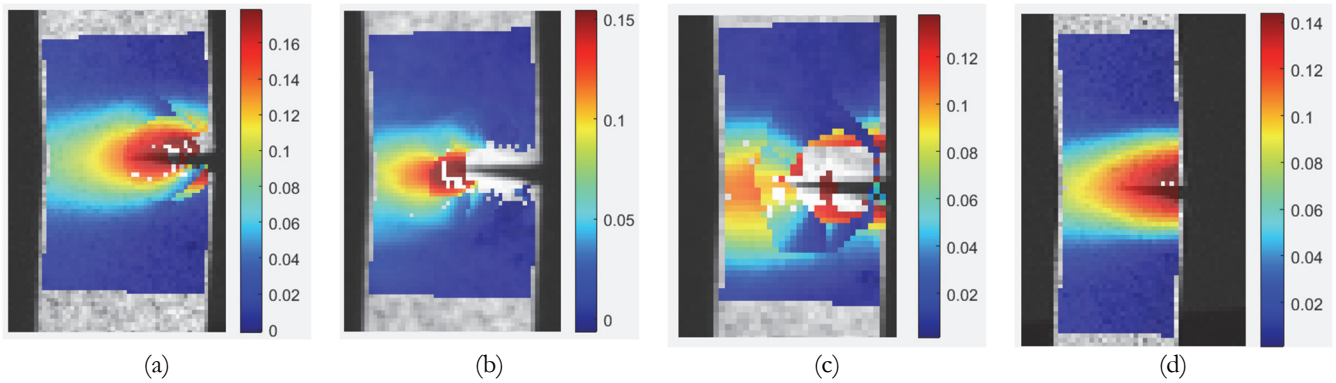

Figure 8: Crack tip location from axial strain field using DIC (a) Original (b) Gaussian filter (c) Median filter (d) Unsharp mask filter

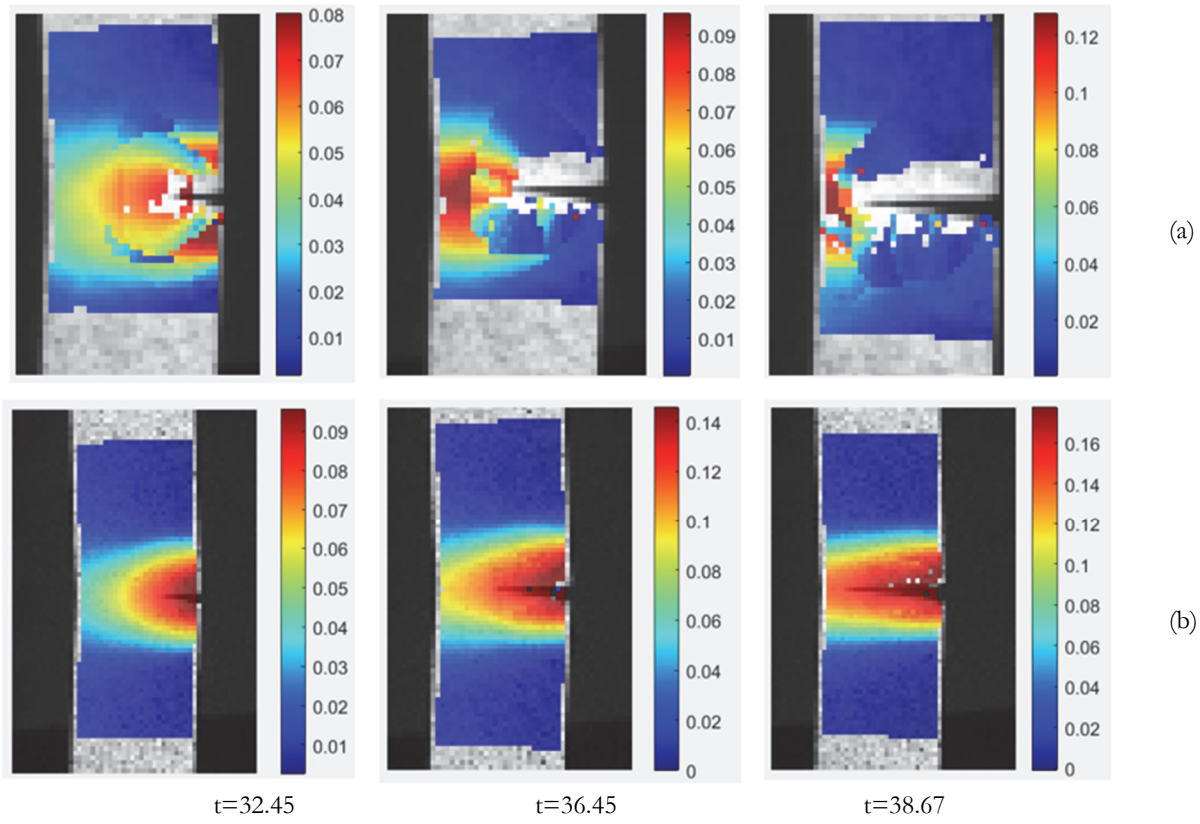

Figure 9: Sequence of images following crack length from axial strain field using DIC (a) Median filter (b) Unsharp mask filter.

Fig. 8 shows excellent compatibility between the visual detection of the crack using ImageJ and the developed algorithm after processing the images using the Gaussian filter. Thus, the applied filter allows tracking the damage in the first propagation zone and removing the limitation due to the noise.

DIC is an effective technique for understanding the failure mechanism with the best-suited filter in terms of simplicity, low cost, and gain time which this method takes less time than the visual method.

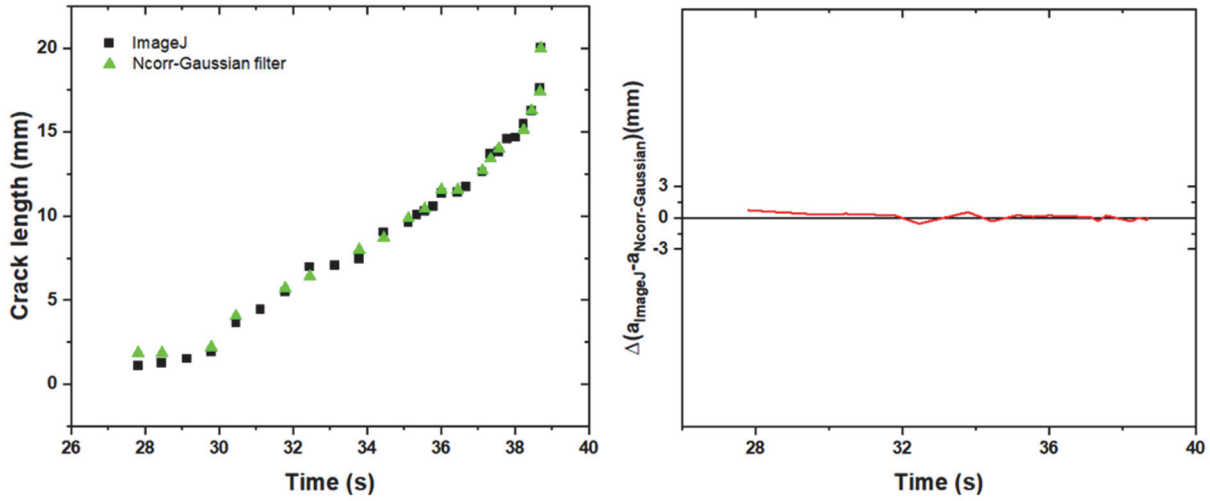

(a) (b)

Figure 8: (a) crack length as a function of time using ImageJ and the developed algorithm with Gaussian filter; (b) Difference between the two graphs.

Conclusion

To investigate the crack tip position, PVC SENT specimens were used. An experimental approach is based on the digital image process proposing two procedures for an accurate crack length. The first procedure proposes an image processing method for detecting cracks to remove all of the light variation and noise to detect the cracks using ImageJ software correctly.

Moreover, the second procedure introduces a new algorithm detecting the crack tip position based on the discontinuity area by utilizing the measured axial deformation exported from the Ncorr program using DIC. However, the noise of the digital images disturbs the DIC measurements near the crack tip, introducing errors at low displacement levels. An image process method is proposed based on filtering images before applying the DIC method using Gaussian, Median, and Unsharp mask filters to overcome this limitation. The principal finding shows excellent compatibility between the visual detection of the crack using ImageJ and the developed algorithm after processing the images using the Gaussian filter. The performance of the Gaussian filter is better than the Median and Unsharp mask filters. Thus, the Gaussian filter allows tracking the damage in the first propagation zone and suppressing the limitation due to the noise. The crack tip position is detected quickly and accurately using the second proposed method, suppressing the problem with the noise distribution.

References

[1] Clark, A.B.J., Irwin, G.R. (1966). Crack-propagation behaviors, Experimental Mechanics 6(6), pp. 321–330. DOI: 10.1007/BF02327512.

[2] Reut, V., Vaysfeld, N., Zhuravlova, Z. (2018). Elastic crack-tip stress field in a semi-strip, Frattura Ed Integrità Strutturale, 12(44), pp. 82–93. DOI: 10.3221/IGF-ESIS.44.07.

[3] Najat, Z., Fatima, M., Rajaa, R., Ibrahim, M., Hassan, R. (2022). PVC failure modelling through experimental and digital image correlation measurements, Frattura Ed Integrità Strutturale, 16(60), pp. 488–503. DOI: 10.3221/IGF-ESIS.60.33.

[4] Ouardi, A., Majid, F., Mouhib, N., Elghorba, M. (2018). Residual life prediction of defected Polypropylene Random copolymer pipes (PPR), Frattura Ed Integrità Strutturale, 12(43), pp. 97–105. DOI: 10.3221/IGF-ESIS.43.07.

[5] Majid, F., Elghorba, M. (2017). HDPE pipes failure analysis and damage modeling, Eng Fail Anal, 71, pp. 157–165. DOI: 10.1016/J.ENGFAILANAL.2016.10.002.

[6] Majid, F., Zekeriti, N., Rhanim, R., Lahlou, M., Rhanim, H., Mrani, B. (2020). Mechanical behavior and crack propagation of ABS 3D printed specimens, Procedia Structural Integrity, 28, pp. 1719–1726. DOI: 10.1016/J.PROSTR.2020.10.147.

[7] Zekriti, N., Rhanim, R., Majid, F., Lahlou, M., Ibrahim, M., Rhanim, H. (2020). Mode I stress intensity factors of printed and extruded specimens based on Digital Image Correlation method (DIC): case of ABS material, Procedia Structural Integrity, 28, pp. 1745–1754. DOI: 10.1016/J.PROSTR.2020.10.149.
[8] Scetta, G., Euchler, E., Ju, J., Selles, N., Heuillet, P., Ciccotti, M., Creton, C. (2021). Self-Organization at the Crack Tip of Fatigue-Resistant Thermoplastic Polyurethane Elastomers, Macromolecules, 54(18), pp. 8726–8737. DOI: 10.1021/ACS.MACROMOL.1C00934/SUPPL_FILE/MA1C00934_SI_001.PDF.
[9] Chen, X., Ye, Z., Xia, J.Y., Wang, J.X., Ji, B.H. (2020). Double-Probe Ultrasonic Detection Method for Cracks in Steel Structure, Applied Sciences 2020, 10(23), 8436. DOI: 10.3390/APP10238436.
[10] Zhao, Y., Chen, J., Sun, J., Song, J., Ma, J., Liu, S., Zhu, Y. (2018). Applications of laser ultrasonic technique on nondestructive testing and evaluation of materials, MATEC Web of Conferences, 173, p. 02033. DOI: 10.1051/MATECCONF/201817302033.
[11] Broberg, P. (2013). Surface crack detection in welds using thermography, NDT and E International, 57, pp. 69–73. DOI: 10.1016/j.ndteint.2013.03.008.
[12] Rasband., S., W. (2012). ImageJ: Image processing and analysis in Java, Ascl, 1206.013.
[13] Mahfuzur Rahman, Md., Saifullah, I., Kumar Ghosh, S. (2019). Detection and Measurements of Cracks in Axially Loaded Tension RC Members by Image Processing Technique, American Journal of Civil Engineering and Architecture, 7(2), pp. 115–120. DOI: 10.12691/ajcea-7-2-5.
[14] Zawad, M., Shahriar, R., Zawad, M., Shahriar, F., Rahman, M. and Priyom, S. N. (2021). A Comparative Review of Image Processing Based Crack Detection Techniques on Civil Engineering Structures. Journal of Soft Computing in Civil Engineering, 5(3), 58-74.
[15] Cinar, A.F., Barhli, S.M., Hollis, D., Flansbjer, M., Tomlinson, R.A., Marrow, T.J., Mostafavi, M. (2017). An autonomous surface discontinuity detection and quantification method by digital image correlation and phase congruency, Opt Lasers Eng, 96, pp. 94–106. DOI: 10.1016/j.optlaseng.2017.04.010.
[16] Sutton, M., Orteu, J., Schreier, H. (2009). Image correlation for shape, motion and deformation measurements: basic concepts, theory and applications.
[17] Chu, T.P., Sutton, M., Chu, T.C., Ranson, W.F., Sutton, M.A., Peters, W.H. (n.d.). Applications of digital-image-correlation techniques to experimental mechanics, Researchgate.Net. DOI: 10.1007/BF02325092.
[18] Helm, J. D., McNeill, S. R. and Sutton, M. A. (1996). Improved three-dimensional image correlation for surface displacement measurement. Optical Engineering, 35(7), 1911-1920.
[19] Sutton, M. A., Wolters, W. J., Peters, W. H., Ranson, W. F. and McNeill, S. R. (1983). Determination of displacements using an improved digital correlation method. Image and vision computing, 1(3), 133-139.
[20] Liu, M., Guo, J., Li, Z., Hui, C. Y. and Zehnder, A. T. (2019). Crack propagation in a PVA dual-crosslink hydrogel: Crack tip fields measured using digital image correlation. Mechanics of Materials, 138, 103158. Blaber, J., Adair, B., Antoniou, A. (2015). Ncorr: Open-Source 2D Digital Image Correlation Matlab Software, Exp Mech, 55(6), pp. 1105–1122. DOI: 10.1007/S11340-015-0009-1.
[21] Ali, M. B., Ab Ghani, A. F., DharMalingam, S. and Mahmud, J. (2016). Digital image correlation (DIC) technique in measuring strain using opensource platform Ncorr. Journal of Advanced Research in Applied Mechanics, 26(1), 10-21.
[22] Pan, B., Asundi, A., Xie, H. and Gao, J. (2009). Digital image correlation using iterative least squares and pointwise least squares for displacement field and strain field measurements. Optics and Lasers in Engineering, 47(7-8), 865-874.
[23] Djouda, J. M., Bouaziz, M. A., Zouaoui, M., Rambaudon, M., Gardan, J., Recho, N. and Crépin, J. (2020). Experimental approach for microscale mechanical characterization of polymeric structured materials obtained by additive manufacturing. Polymer Testing, 89, 106634.
[24] Marae Djouda, J., Bouaziz, M.A., Zouaoui, M., Rambaudon, M., Gardan, J., Recho, N., Crépin, J. (2020). Experimental approach for microscale mechanical characterization of polymeric structured materials obtained by additive manufacturing, Polym Test, 89. DOI: 10.1016/j.polymertesting.2020.106634.
[25] Bouaziz, M. A., Marae-Djouda, J., Zouaoui, M., Gardan, J. and Hild, F. (2021). Crack growth measurement and J-integral evaluation of additively manufactured polymer using digital image correlation and FE modeling. Fatigue & Fracture of Engineering Materials & Structures, 44(5), 1318-1335.
[26] Ruocci, G., Rospars, C., Moreau, G., Bisch, P., Erlicher, S., Delaplace, A., Henault, J.M. (2016). Digital Image Correlation and Noise-filtering Approach for the Cracking Assessment of Massive Reinforced Concrete Structures, Strain, 52(6), pp. 503–521. DOI: 10.1111/str.12192.
[27] Boyat, A.K., Joshi, B.K. (2015). A Review Paper: Noise Models in Digital Image Processing, Signal Image Process, 6(2), pp. 63–75. DOI: 10.5121/sipij.2015.6206.

[28] Wang, Y. Q., Sutton, M. A., Bruck, H. A. and Schreier, H. W. (2009). Quantitative error assessment in pattern matching: effects of intensity pattern noise, interpolation, strain and image contrast on motion measurements. Strain, 45(2), 160-178.

[29] Baldoni, J., Lionello, G., Zama, F., Cristofolini, L. (2016). Comparison of different filtering strategies to reduce noise in strain measurement with digital image correlation, Journal of Strain Analysis for Engineering Design, 51(6), pp. 416–430. DOI: 10.1177/0309324716646690.

[30] Kumar, M., Tounsi, Y., Kaur, K., Nassim, A., Mandoza-Santoyo, F., Matoba, O. (2020). Speckle denoising techniques in imaging systems, Journal of Optics, 22(6), p. 063001. DOI: 10.1088/2040-8986/AB8B7F.

[31] Rueden, C.T., Schindelin, J., Hiner, M.C., DeZonia, B.E., Walter, A.E., Arena, E.T., Eliceiri, K.W. (2017). ImageJ2: ImageJ for the next generation of scientific image data, BMC Bioinformatics, 18(1). DOI: 10.1186/S12859-017-1934-Z.